Supporting Information

Gorgun et al. 10.1073/pnas.0901166106

SI Text

Animals, Disease Detection and Infusion of CLL Cells. Mice were examined for lymphadenopathy and splenomegaly and at specific ages or when visibly ill, mice were killed and hematopoietic tissues including spleen, lymph nodes, bone marrow, peripheral blood, and liver were extracted. Splenic mononuclear cells were separated by ficoll-hypaque centrifugation and cells were labeled with anti-mouse CD5 PE, CD19 CYT, IgM FITC, and IgD FITC, Igκ FITC, and Igλ FITC monoclonal antibodies. Three-month-old Eμ-*TCL1* mice that had not developed CLL were infused (i.v. injection) with 50×10^6 splenic mononuclear cells (≥98% CD5+CD19+Igκ+ or Igλ+) in 0.5 ml PBS into the tail vein on days 0 and 3, and spleens removed at day 8. CLL cells were obtained from Eμ-*TCL1* mice over 12 months of age with disease.

Antibodies and Reagents. Rhodamine Phalloidin, CellTracker Blue CMAC, and Alexa Fluor 488-labeled goat anti-rabbit IgG antibodies were all purchased from Invitrogen. Anti-Cdc42 and anti-Lck were from Santa Cruz Biotechnology. Anti-phosphotyrosine, clone 4G10 (FITC conjugate) was purchased from Millipore. All other reagents were purchased from Sigma unless otherwise stated.

Gene-Chip Array and Expression-Data Analysis. Quality control of the RNA samples was performed by spectrophotometric analysis and size fractionation (Agilent Technologies). RNA conversion of cDNA and subsequent hybridization to gene arrays was performed in the Core Facility at the Dana-Farber Cancer Institute, according to the manufacturer's protocols (Affymetrix). CEL files have been deposited into the Gene Expression Omnibus and are available with accession numbers GSE8835 for human data (http://www.ncbi.nlm.nih.gov/geo/info/linking.html) GSE8836 for murine data (http://www.ncbi.nlm.nih.gov/geo/info/linking.html).

Data were normalized using DNA-Chip Analyzer (dChip) to obtain perfect-match-only model-based expression intensities. An array with a median overall intensity was chosen as the baseline array against which other arrays were normalized at probe-intensity level. dChip was used to perform unsupervised analysis by gene filtering, excluding genes that lacked sufficient variability across groups, and hierarchical clustering of genes and samples. The filtering criteria required that a gene's coefficient of variation across all samples (after pooling replicate arrays) be between 0.9 and 2.0 and that a gene be called "present" in more than 20% of the arrays. Hierarchical clustering was performed using the distant metric 1-correlation (Pearson): that is, the distance between 2 genes is defined as $1-r$, where r is the Pearson correlation coefficient between the standardized expression values (mean 0 and SD 1) of the 2 genes across the samples and centroid linkage. The expression levels for each gene was standardized to mean 0 and SD 1, with the standardized expression values falling within [–3, +3]. To identify the genes whose expression patterns best distinguished groups, the permutation distribution of the maximum t-statistic was analyzed using Permax. The custom program written for R software by Robert Gray calculates Permax values and is available free on-line (http://biowww.dfci.harvard.edu/~gray/permax.html). For CD4 and CD8 T-cell groups, we compared gene-expression profiles using the Permax test according to cell purity (< 85% vs. ≥ 85%), age (< 12 months old vs. ≥ 12 months old), CLL cell content (< 40% vs. ≥ 40%) and gender (female vs. male). In these supervised analyses, to control the overall error rate, the Permax P-value was calculated by comparing the observed t-statistics for each gene from their log values to the permutation distribution of the largest t-statistic obtained over the 45,037 genes. For each gene, the P-value is the proportion of permutations with the maximum t-statistics over all genes greater or equal to the observed value for a particular gene. Differentially expressed genes (filtered by $P \leq 0.05$ and $1.2<\text{fold} \geq 1.2$) from supervised analyses by their involvement in specific cellular pathways were determined using gene microarray pathway profiler 2.0 (GenMapp) software. Fisher t-test analysis was used to determine over-represented cellular pathways ($P \leq 0.05$). The comparison of overlapping genes obtained by supervised analyses between our human gene-expression profiles (Affymetrix hu133A and mouse gene-expression profiles (Affymetrix moe430.2) was performed using RESOURCERER, a database for annotating and linking microarray resources within and cross species.

Quantitative RT-PCR and Western Immunoblot. Total cell protein was extracted from ≥ 99% pure splenic CD4 T or CD8 T cells and protein blots performed with primary antibodies against rabbit mouse polyclonal antibodies Lyn and PI3K (Santa Cruz Biotechnology) and then labeled with secondary antibody HRP-conjugated goat anti rabbit Ig and detected by Western blot chemiluminescence reagents (Perkin–Elmer). Expression levels normalized with β-Actin (Santa Cruz Biotechnology) and measured using Kodak Digital Science Image Station-440CF luminometer (Eastman Kodak).

Immune Assessment. For CTL effector assays, CD8 cells from WT and Eμ-*TCL1* mice with and without CLL (6 animals per group) were stimulated in vitro with monocyte derived dendritic cells pulsed with Ig heavy chain- (*IgVH*) derived peptide GSAINYAPSI weekly for 4 weeks. Killing of CLL cells expressing this *IgVH* by the resulting T-cell lines was assessed at the effector-:target ratios shown from WT and Eμ-*TCL1* mice with and without CLL. For in vivo antigen-specific T-cell activation assays, WT and Eμ-*TCL1* mice with and without CLL were immunized with gp33 peptide KAVYNFATM. On day 8 spleen cells from immunized mice (9 in each group) were stimulated with indicated concentrations of KAVYNFATM peptide in 96-well plates in triplicates. Proliferation was assayed after 3 days of treatment by [^{3}H]-Thymidine incorporation, measured by β-scintillation counter. For proliferation assays, mononuclear cells from Eμ-*TCL1* mice with and without CLL were stimulated in triplicate with 100-ng/ml phorbol myristate acetate and 4-μg/ml ionomycin for 3 days. Next, 1 μCi per well [^{3}H]-Thymidine was added to each triplicate 18 h before harvesting and proliferation measured by β-scintillation counter.

Cell Conjugation Assays. Healthy or malignant B cells (2×10^6 healthy WT B cells or CLL cells) were stained with CellTracker Blue CMAC (7-amino-4-chloromethylcoumarin) following the manufacturer's instructions and pulsed with or without 2 μg/ml of a mixture of staphylococcal superantigens (SEA and SEB; Sigma) for 30 min at 37 °C. B cells were centrifuged ($200 \times g$ for 5 min) with an equal number of T cells, incubated at 37 °C for 10 min (CD8 T cells) or 15 min (CD4 T cells). Phosphotyrosine and Lck were assessed at 5-min conjugation times, then plated (centrifuged) onto polyL-lysine-coated coverslips and fixed for 15 min at room temperature with 3% methanol-free formaldehyde in PBS.

Immunofluorescence and Confocal Microscopy Image Acquisition. F-actin was stained with rhodamine phalloidin (Invitrogen). CD8 T-cell conjugates formed during 5 min were stained for Lck. CD4 T-cell conjugates formed during 15 min were stained for Cdc42. Medial optical section images were captured with a Zeiss 510 confocal laser-scanning microscope using a 63× objective. Detectors were set to detect an optimal signal below the saturation limits. Image sets to be compared were acquired during the same session and using the same acquisition settings.

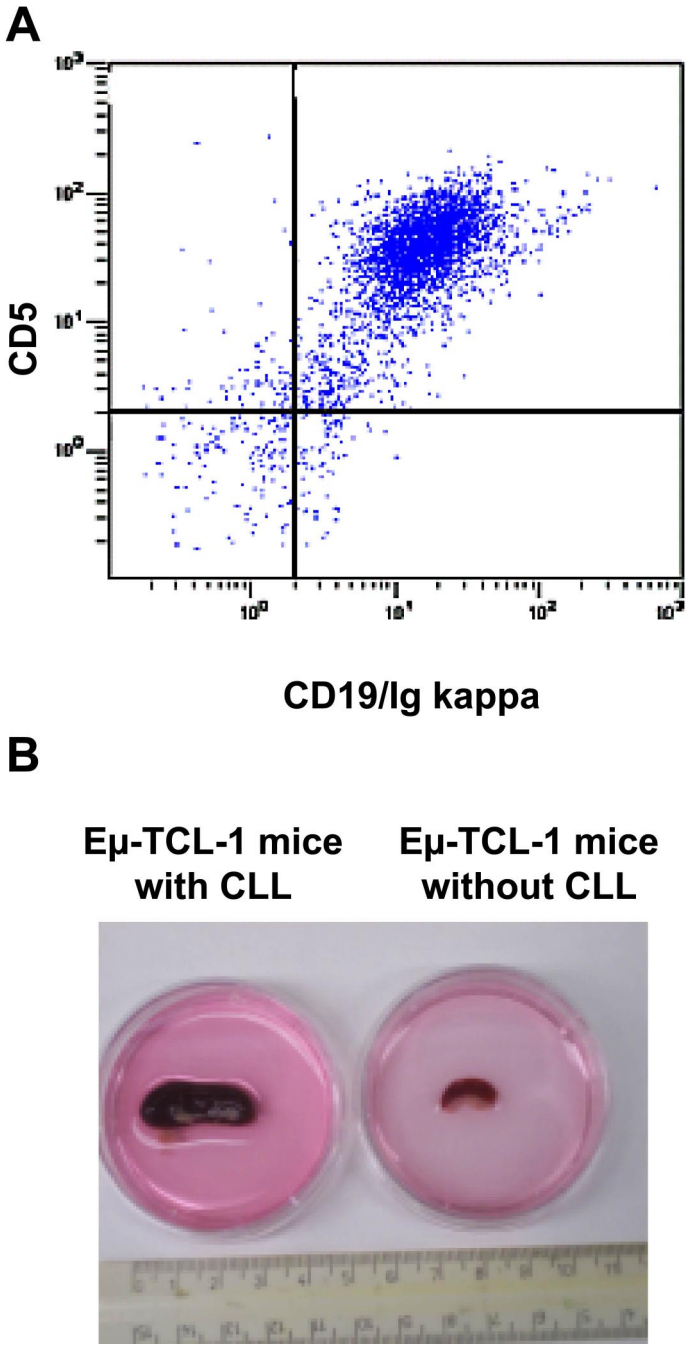

Fig. S1. Phenotypic characteristics of CLL cells in Eμ-*TCL1* mice. (*A*) Development of CLL disease was demonstrated by increased $CD5^{+}CD19^{+}$Ig (κ or λ) coexpression B cells in $\geq$ 12-month-old Eμ-*TCL1* mice. Data represents phenotypic characteristics of 12 Eμ-*TCL1* mice. (*B*) Enlargement in spleen from $\geq$ 12-month-old Eμ-*TCL1* mouse with CLL compared to $<$ 12-month-old Eμ-*TCL1* mouse without CLL.

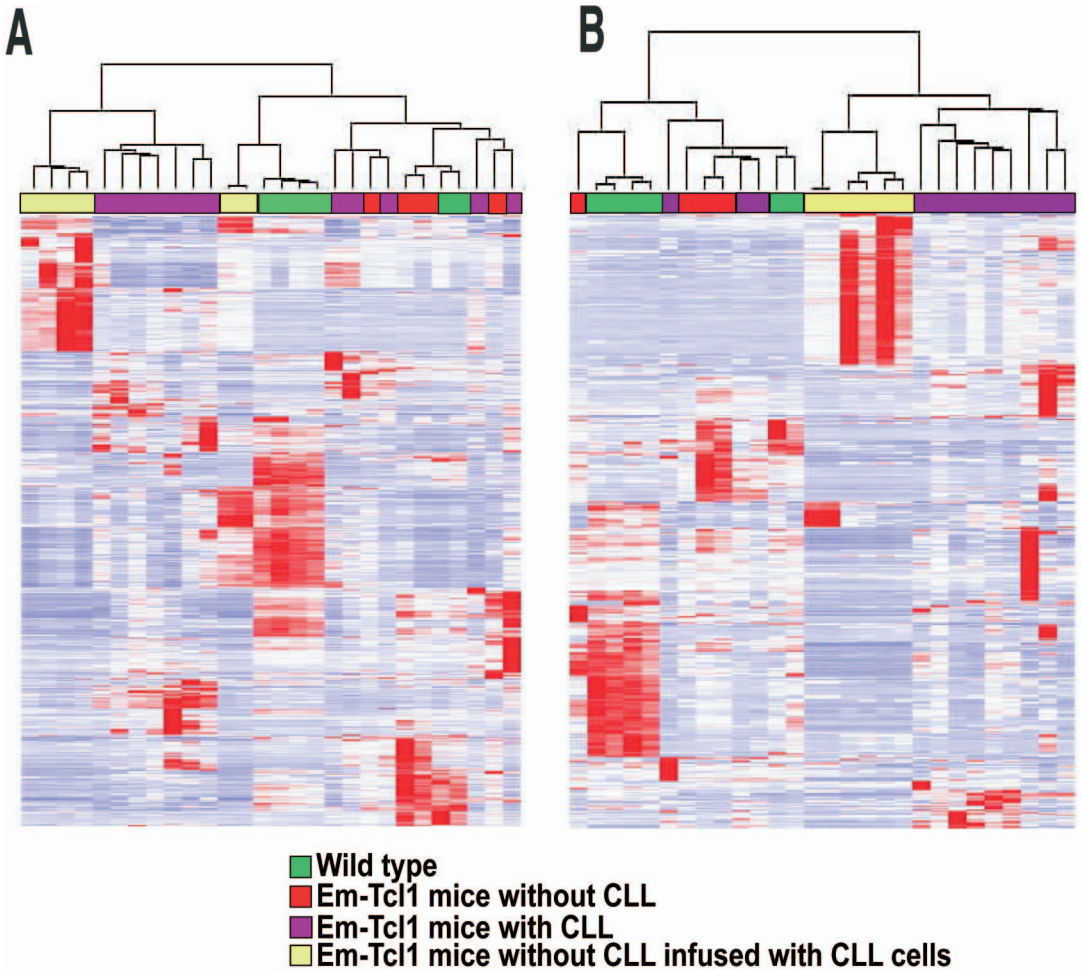

Fig. S2. CLL induces changes in gene-expression profiles in T cells from Eμ-*TCL1* mice. Hierarchical clusters of (*A*) CD4 T cells and (*B*) CD8 T cells from WT mice ($n = 6$), Eμ-*TCL1* mice with CLL ($n = 12$), or young mice infused with CLL cells ($n = 6$) compared to Eμ-*TCL1* mice without CLL ($n = 4$) using dCHIP to perform an unsupervised statistical analysis as described in *Materials and Methods*.

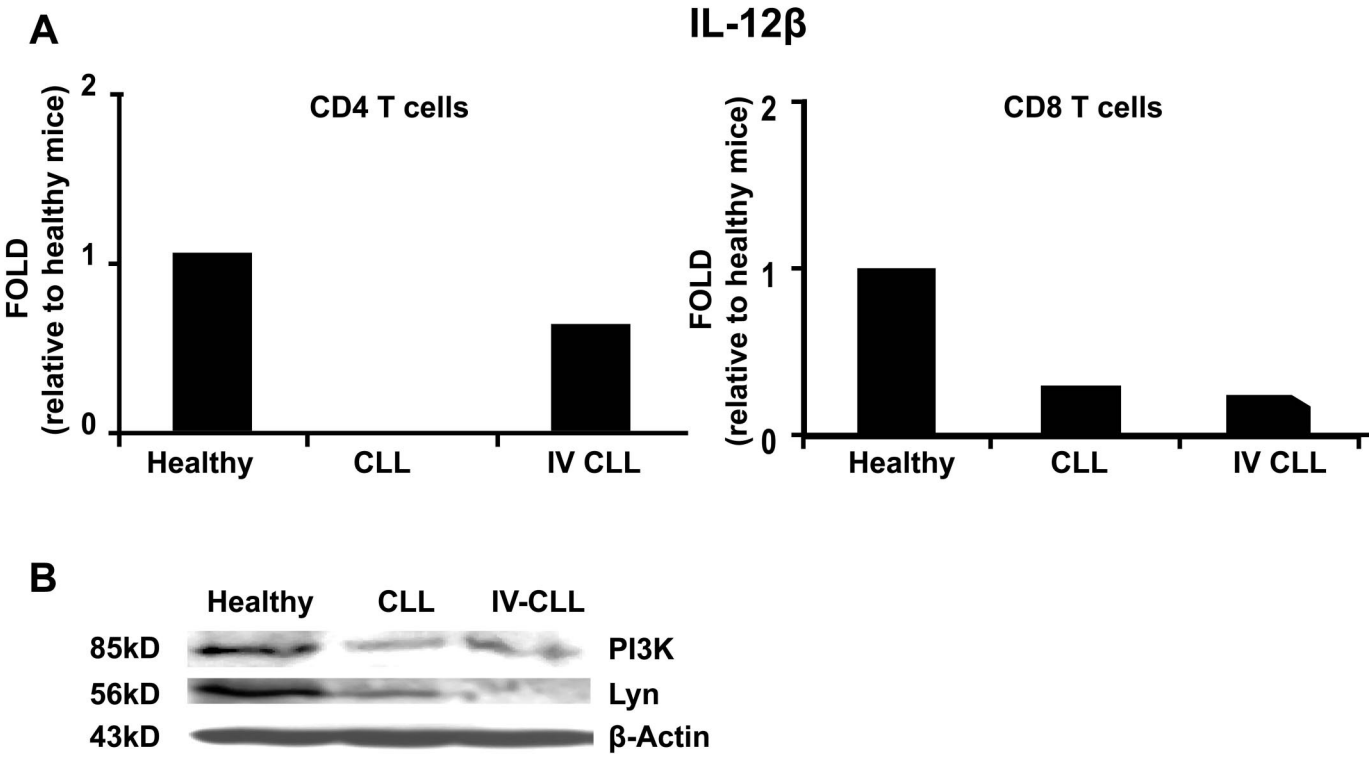

Fig. S3. CLL cells induce in vivo molecular and protein expression changes in CD4 and CD8 T cells from Eμ-*TCL1* mice with CLL and after infusion (i.v. injection, IV) of CLL cells in young mice. (*A*) Quantitative RT-PCR analysis confirmed gene-expression changes seen on the microarrays, represented here by decreased expression of *Il12β* in both CD4 and CD8 T cells from mice with CLL (CLL) and young mice infused with CLL cells (IV-CLL) compared to WT mice. The results represent fold-difference of the mean of triplicates relative to mean *GAPDH* expression and is representative of 3 experiments performed. (*B*) Western blot analysis confirmed changes in protein expression were consistent with the altered gene-expression profiles, as shown here with decreased expression of PI3K and Lyn proteins in $CD4^+$ T cells. The figure is representative of 3 independent experiments performed. (*C*) Immunophenotypic changes in protein expression confirmed changes in gene-expression profiling. Shown here is decreased expression of CD28 and BTLA and increased expression of CD25 and CTLA-4 in CD4 T cells from mice with CLL (*Middle*) or young mice infused with CLL (*Right*). Age-matched WT mice were used as comparative controls (*Left*). The expression levels were measured using flow cytometry as % cells/10,000 cell count. Figure plots shown are representative of 3 independent experiments.

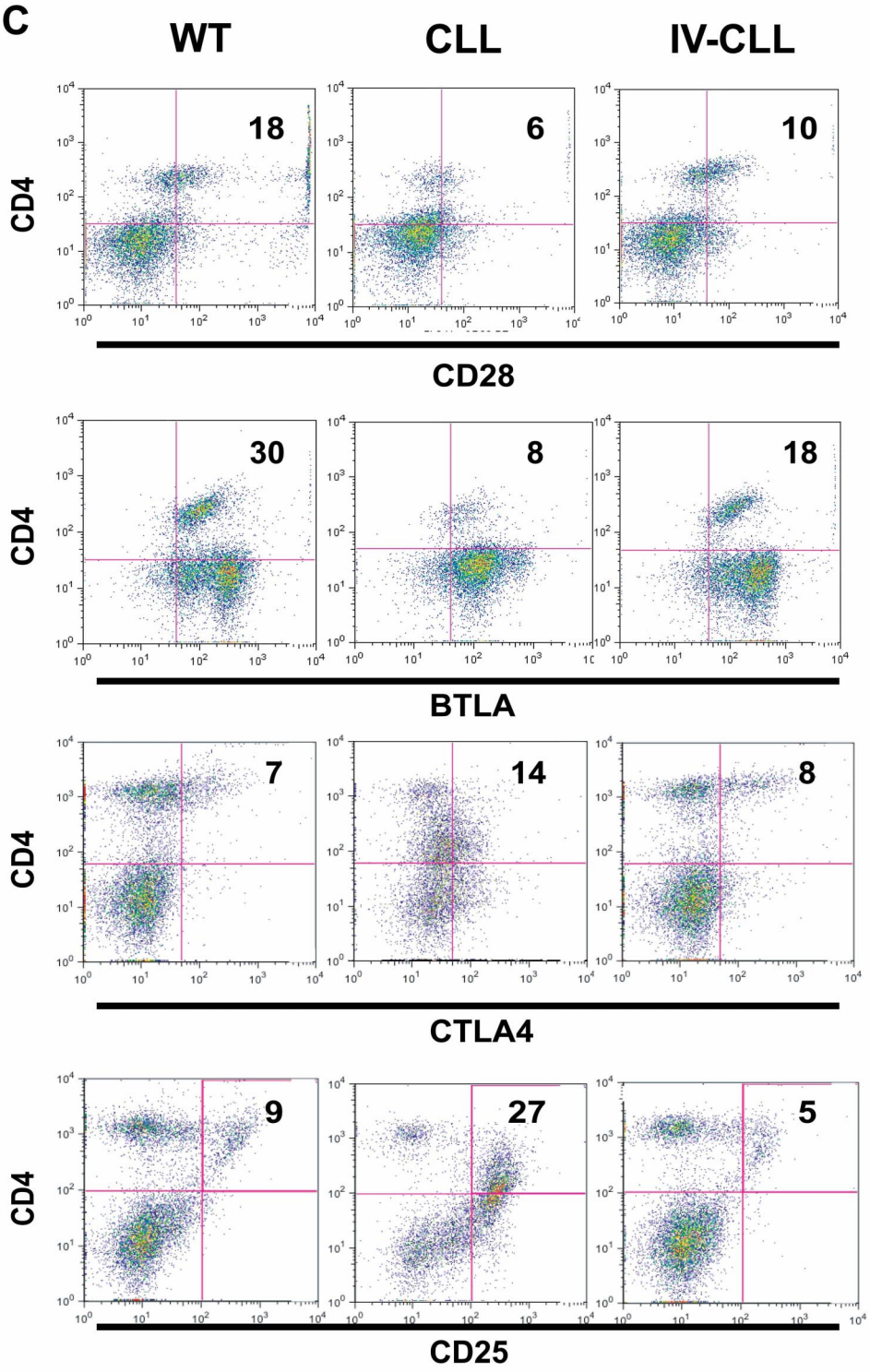

Fig. S3. continued.

Table S1. Classification of differentially expressed genes in CD4 T cells by their involvement in specific signaling pathways

Pathway	Probe set ID	Gene name	Gene symbol	Fold (CLL vs. healthy)
A. MAPK-dependent cell proliferation pathway	1450194_a_at	Myb proto-oncogene protein	*Myb*	1.99
	1419334_at	Cytotoxic T lymphocyte associated protein 4	*CTLA4*	1.26
	1425396_a_at	Lymphocyte protein tyrosine kinase	*Lck*	2.91
	1417597_at	CD28 antigen	*CD28*	−1.7
	1455656_at	B and T lymphocyte attenuator	*BTLA*	−2.13
	1448600_s_at	Vav3 oncogene	*Vav3*	−1.62
	1437861_s_at	Protein kinase C, epsilon	*Pkce*	−1.53
	1420710_at	Reticuloendotheliosis oncogene	*Rel*	−3
	1449773_s_at	Growth arrest and DNA-damage-inducible 45 beta	*Gadd45b*	−1.71
	1451318_a_at	Yamaguchi sarcoma viral (v-yes-1) oncogene homolog	*Lyn*	−1.66
	1416351_at	Mitogen activated protein kinase kinase 1	*Map2k1*	−1.37
	1451979_at	Kirsten rat sarcoma oncogene 2	*Kras2*	−1.47
	1417398_at	Related RAS viral (r-ras) oncogene homolog 2	*Rras2*	−1.72
	1426759_at	Mitogen activated protein kinase kinase kinase kinase 3	*Map3k3*	−1.75
	1451462_a_at	Interferon (alpha and beta) receptor 2	*Ifnar2*	−1.59
	1419169_at	mitogen-activated protein kinase 6	*Mapk6*	−4.72
	1422134_at	FBJ osteosarcoma oncogene B	*Fosb*	−1.98
	1418971_x_at	B-cell leukemia/lymphoma10	*Bcl10*	−1.77
	1448694_at	Jun oncogene	*Jun*	−1.82
	1427705_a_at	Nuclear factor kappa-b1	*Nfkb1*	−1.4
Ras-dependent Th cell differentiation pathway	1420895_at	Transforming growth factor, beta receptor I	*Tgfbr1*	−2.15
	1426397_at	Transforming growth factor, beta receptor II	*Tgfbr2*	−1.45
	1422286_a_at	Transforming growth factor B induced factor	*Tgif*	−3.2
	1426373_at	Sloan-Kettering viral oncogene homolog	*Ski*	−1.5
	1422054_a_at	SKI-like	*Skil*	−2.3
	1435224_at	CREB binding protein	*Crebbp*	−1.7
	1423389_at	Mad homolog 7(Madh7)	*Smad7*	−2.2
Cytokine/chemokine response pathway	1423558_at	Interferon gamma receptor 2	*Ifngr2*	−2
	1419530_at	Interleukin 12b	*Il12b*	−3.71
	1460669_at	Interleukin enhancer binding factor 3	*Ilf3*	−1.59
	1458364_s_at	Interferon alpha responsive gene	*Ifrg15*	−1.7
	1421174_at	Interferon regulatory factor 4	*Irf4*	−1.77
	1438629_x_at	Granulin	*Grn*	−2.85
	1419083_at	Tumor necrosis factor (ligand) superfamily, member 11	*Tnfsf11*	−2.16
	1448710_at	Chemokine (C-X-C) motif receptor 4	*Cxcr4*	−2.3

Differentially expressed genes involved in MAPK-dependent cell proliferation and actin cytoskeletal formation, ras-dependent (Th cell differentiation) and cytokine/chemokine response pathways in CD4 T cells from Eμ-*TCL1* mice with CLL or young mice infused with CLL cells compared to Eμ-*TCL1* mice without CLL are represented by selected genes. Increased gene expression (+Fold) and decreased gene expression (–Fold) in T cells from CLL compared to healthy mice.

Table S2. Classification of differentially expressed genes in CD8 T cells by their involvement in specific signaling pathways

Pathway	Probe set ID	Gene name	Gene symbol	Fold (CLL vs healthy)
Vesicle-trafficking, cytoskeleton organization, intracellular transport and cell motility pathways	1421546_a_at	Rac GTPase-activating protein 1	*Racgap1*	1.9
	1429123_at	Member of RAS oncogene family	*Rab27a*	2.4
	1449259_at	Member of RAS oncogene family	*Rab3d*	2.1
	1433436_s_at	Adaptor protein complex AP-1, gamma 2 subunit	*Ap1 g2*	1.9
	1422593_at	Adaptor-related protein complex 3, sigma 1 subunit	*Ap3 s1*	1.8
	1415698_at	Golgi phosphoprotein 2	*Golph2*	1.5
	1430522_a_at	Vesicle-associated membrane protein 5	*Vamp5*	1.4
	1416082_at	Member of RAS oncogene family	*Rab1*	−1.5
	1423083_at	Member of RAS oncogene family	*Rab33b*	−1.8
	1417622_at	Solute carrier 12 member 2	*Slc12a2*	−2.0
	1416465_a_at	Vesicle-associated membrane protein-associated protein A	*Vapa*	−1.5
	1451979_at	Kirsten rat sarcoma oncogene 2	*Kras2*	−1.5
	1435807_at	Cell division cycle 42	*Cdc42*	−1.6
	1460419_a_at	Protein kinase C, beta	*Pkcb*	−1.5
Cytokine-Chemokine regulation pathways	1421291_at	Interleukin 18 receptor accessory protein	*Il18rap*	1.9
	1421188_at	Chemokine (C-C) receptor 2	*Ccr2*	1.9
	1424244_at	Intercellular adhesion molecule	*Icam1*	1.5
	1417932_at	Interleukin 18	*Il18*	−2.7
	1429559_at	Guanine nucleotide binding protein alpha q polypeptide	*Gnaq*	−2.1
	1422555_s_at	Guanine nucleotide binding protein, alpha 13	*Gna13*	−1.9
	1417379_at	IQ motif containing GTPase activating protein 1	*Iqgap1*	−1.4
	1460352_s_at	Phosphatidylinositol 3 kinase, regulatory subunit, polypeptide 4, p150	*Pik3r4*	−1.9
	1421023_at	Phosphatidylinositol 3-kinase, C2 domain containing, alpha polypeptide	*Pik3c2a*	−1.8
	1419279_at	Phosphatidylinositol-4-phosphate 5-kinase, type II, alpha	*Pip5k2a*	−1.5
	1423182_at	Tumor necrosis factor receptor superfamily, member 13b	*Tnfrsf13b*	−2.3
	1415989_at	Vascular cell adhesion molecule 1	*Vcam1*	−3.2
	1419128_at	Integrin alpha X	*Itgax*	−1.7
	1419530_at	Interleukin 12b	*Il12b*	−7.9
	1418718_at	Chemokine (C-X-C motif) ligand 16	*Cxcl16*	−2.4
	1418652_at	Chemokine (C-X-C motif) ligand 9	*Cxcl9*	−2.3

Differentially expressed genes involved in cytoskeleton organization, vesicle trafficking, intracellular transport, cell motility and cytokine-chemokine regulation pathways in CD8 T cells from Eμ-*TCL1* mice with CLL or young mice infused with CLL cells compared to Eμ-*TCL1* mice without CLL are represented by selected genes. Comparison of expression levels between Eμ-*TCL1* mice with CLL, young mice infused with CLL cells, and Eμ-*TCL1* mice without CLL were detected using a supervised analysis ($P \leq 0.05$). Increased gene expression (+Fold) and decreased gene expression (–Fold) in T cells from CLL compared to healthy mice.

Table S3. Characteristics of mice used for the gene-expression profiling studies

Mice			Gender				
Wild type	Eμ-*TCL1*	Eμ-*TCL1* injected with CLL cells	Male	Female	Age, month	Tumor cells, %	T cell purity, %
6	16	6	12	16	3–18.5	10–93	66–99

TCL1 gene transgenic B6C3 mice (Eμ-*TCL1*) ($n = 16$) were examined for lymphadenopathy and splenomegaly to detect for CLL development. At different ages (3–18.5 months old) and visibly ill, mice were killed to obtain hematopoietic tissues, including spleen, lymph nodes, bone marrow, peripheral blood, and liver. To analyze the in vivo impact of CLL cells on T cells, Eμ-*TCL1* mice without CLL ($n = 6$) were infused (intravenous injection) with splenic mononuclear cells with a high number of CLL cells ($\geq$98% $CD5^+CD19^+$Ig light $chain^+$ B cells). Confirmation that no CLL was seen in young mice was assessed by immunophenotyping of peripheral blood samples. Age-matched WT (B6C3) mice ($n = 6$) were used as controls.